

# Integrated ramp metering and lane-changing feedback control at motorway bottlenecks

Farzam Tajdari<sup>1</sup>, Claudio Roncoli<sup>1</sup>, Nikolaos Bekiaris-Liberis<sup>\*2</sup>, and Markos Papageorgiou<sup>3</sup>

**Abstract**—Considering the target of an operating effectively transportation system, we propose here a novel methodology for integrated lane-changing and ramp metering control that exploits the presence of connected and partly automated vehicles. In particular, we assume that a percentage of vehicles can receive and implement specific control tasks (e.g., lane-changing commands). A novel approach is designed to robustly maximise the throughput at motorway bottlenecks employing a Linear Quadratic Integral (LQI) regulator in combination with an anti-windup scheme, based on a simple Linear Time Invariant (LTI) model. The method is evaluated via simulation experiments, performed on a first-order, multi-lane, macroscopic traffic flow model, also featuring the capacity drop phenomenon, which allows to demonstrate the effectiveness of the developed methodology and to highlight the improvement in terms of traffic efficiency.

## I. INTRODUCTION

In the last decades, a significant and increasing interdisciplinary effort by the automotive industry, as well as by numerous research institutions around the world, has been devoted to planning, developing, testing, and deploying new technologies that are expected to revolutionise the features and capabilities of individual vehicles in the future [1]. Among the wide range of available systems, few may actually have a direct impact on traffic flow, while the majority of them aims at primarily improving safety or driver's convenience ([2], [3], [4]). In the context of automated and connected vehicles or Automated Highway Systems, only a limited number of works have considered to optimize lane distribution ([5], [6], [7], [8], [9], [10]). A number of other works addressed specifically the problem of deciding on efficient vehicle lane-paths for a motorway under fully automated (AHS) or semi-automated driving (e.g., [5], [6]).

An optimal feedback control strategy [11] for lane-changing control is formulated in [9] as a linear quadratic regulator (LQR) and is extended in [10], to achieve different traffic density distribution for the various lanes at the bottleneck area. However, in both works, it is assumed that another controller ensures that the overall traffic flow entering the area where lane-changing control is applied,

does not significantly exceed the bottleneck capacity. This paper extends the results in [9] presenting a novel methodology for integrated lane-changing and ramp metering control, considering the presence of partly automated and connected vehicles. In particular, it is assumed that equipped vehicles have the capability of bidirectional communication with the infrastructure (V2I); appropriate control actions are decided in a centralised manner by a Traffic Management Center (TMC) and are dispatched to specific vehicles for implementation (e.g., [12], [7]).

The paper is structured as follows: Section II describes the proposed LTI model. In Section III, the controller design is presented. Section IV introduces the experiment setup, while in Section V the obtained simulation results are presented and compared with a reference no-control case. Section VI concludes the paper, highlighting its main results.

## II. LINEAR MULTI-LANE TRAFFIC FLOW MODEL

We consider a multi-lane motorway that is subdivided into  $N$  segments, indexed by  $i = 0, \dots, N$ , of length  $L_i$ , while each segment is composed of lanes, indexed by  $j = m_i, \dots, M_i$ , where  $m_i$  and  $M_i$  are the minimum and maximum indexes of lanes for segment  $i$  denotes each element of the resulting grid (see Fig. 1) as “cell”, which is indexed by  $(i, j)$ . In order to account for any possible network topology, including lane-drops and lane-additions, both on the right and on the left sides of the motorway, we assume that  $j = 0$  corresponds to the segment(s) including the right-most lane. For example, looking at the hypothetical motorway stretch depicted in Fig. 1,  $m_0 = 0$  and  $M_0 = 4$ , while  $m_3 = 1$  and  $M_3 = 3$ .

The model is formulated in discrete time, considering the discrete time step  $T$ , indexed by  $k = 0, 1, \dots$ , where the time is  $t = kT$ . According to this definition, the total number of cells is  $H = \sum_{r=0}^N (M_r - m_r + 1)$  and the number of cells at the bottleneck area is  $S = M_N - m_N + 1$ .

Each motorway cell  $(i, j)$  is characterised by the traffic density  $\rho_{i,j}(k)$ , defined as the number of vehicles present within the cell at time instant  $k$  divided by  $L_i$ . Density dynamically evolves according to the following conservation law equation, see, e.g. [7],

$$\begin{aligned} \rho_{i,j}(k+1) = & \rho_{i,j}(k) + \frac{T}{L_i} [q_{i-1,j}(k) - q_{i,j}(k)] \\ & + \frac{T}{L_i} [f_{i,j-1}(k) - f_{i,j}(k)] + \frac{T}{L_i} d_{i,j}(k) + \frac{T}{L_i} r_{i,j}(k), \end{aligned} \quad (1)$$

where  $q_{i,j}(k)$  is the longitudinal flow leaving cell  $(i, j)$  and entering cell  $(i+1, j)$  during time interval  $(k, k+1]$ ;  $f_{i,j}(k)$

<sup>1</sup>Department of Built Environment, School of Engineering, Aalto University, Espoo 02150 Finland farzam.tajdari@aalto.fi, claudio.roncoli@aalto.fi

<sup>2</sup>Department of Electrical & Computer Engineering and Production Engineering & Management, Technical University of Crete, Chania 73100, Greece bekiaris-liberis@ece.tuc.gr

<sup>3</sup>School of Production Engineering & Management, Technical University of Crete, Chania 73100, Greece markos@dssl.tuc.gr

\*Nikolaos Bekiaris-Liberis was supported by the funding from the European Commission's Horizon 2020 research and innovation programme under the Marie Skłodowska-Curie Grant Agreement No. 747898, project PADECOT.

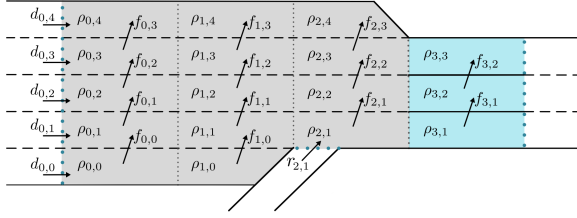


Fig. 1: A hypothetical motorway stretch.

is the net lateral flow moving from cell  $(i, j)$  to cell  $(i, j+1)$  during time interval  $(k, k+1]$ ; and  $d_{i,j}(k)$  is any external flow entering the network in cell  $(i, j)$ , either from upstream of the considered stretch or from an on-ramp, during time interval  $(k, k+1]$ . Since a ramp is assumed to be controlled, we introduce  $r_{i,j}(k)$  as the flow allowed to enter the network from the ramp located in  $(i, j)$  during time interval  $(k, k+1]$  (e.g.,  $r_{2,1}$  in Fig. 1). Depending on the network topology, some terms of (1) may not be present. In particular, the inflow  $q_{i-1,j}(k)$  does not exist for the first segment of the network, the outflow  $q_{i,j}(k)$  does not exist for the last segment before a lane-drop, while lateral flow terms  $f_{i,j}(k)$  exist only for  $m_i \leq j < M_i$ . Following previous considerations, the total number of lateral flow terms is  $F = H - N$ .

Let us consider the well-known relation

$$q_{i,j}(k) = \rho_{i,j}(k) v_{i,j}(k). \quad (2)$$

Since the controller is designed to operate in (and in fact maintain) congestion-free traffic conditions, we assume that the speed in all cells remains at a constant value (e.g., the critical speed)  $v_{i,j}(k) \equiv \bar{v}_{i,j}, \forall i, j, k$ . Despite this may appear a strong assumption, we will see in simulation (Section V) that the controller achieves good performance also when speed varies over time. We therefore replace (2) into (1) and we can write the resulting system in the form of a Linear Time Invariant (LTI) system

$$\bar{x}(k+1) = \bar{A}\bar{x}(k) + \bar{B}u(k) + \bar{d}(k) \quad (3)$$

where (time index  $k$  is omitted to simplify notation)

$$\bar{x} = [\rho_{0,m_0} \dots \rho_{0,M_0} \ \rho_{1,m_1} \dots \rho_{N,M_N}]^T \in \mathbb{R}^H, \quad (4)$$

$$\bar{d} = \left[ \frac{T}{L_0} d_{0,m_0} \dots \frac{T}{L_0} d_{0,M_0} \ \frac{T}{L_0} d_{1,m_1} \dots \frac{T}{L_0} d_{N,M_N} \right]^T \in \mathbb{R}^H, \quad (5)$$

$$u = [f_{0,m_0} \dots f_{0,M_0} \ f_{1,m_1} \dots f_{N,M_N}, r_{i,j}]^T \in \mathbb{R}^{F+1}. \quad (6)$$

Variables  $u$  and  $\bar{d}$  are the controlled and uncontrolled inputs, respectively;  $u$  includes all the lateral flows  $f_{i,j}$  and the ramp flow  $r_{i,j}$  that is assumed controllable, while  $\bar{d}$  includes the external flows that are not in  $u$ . Matrix  $\bar{A} \in \mathbb{R}^{H \times H}$ , composed of elements  $a_{\bar{p},\bar{s}}$ , which reflects the connections between pairs of subsequent cells via a longitudinal flow. Finally, matrix  $\bar{B}$ , composed of elements  $b_{\bar{p},\bar{s}}$  which reflects the interconnections among cells via their entering or leaving lateral flows. Thus, the matrices for the mentioned system can be described as

$$a_{\bar{p},\bar{s}} = \begin{cases} 1 & \text{if } \bar{p} = \bar{s} \text{ and } (j < m_{i+1} \text{ or } j > M_{i+1}) \\ 1 - \frac{T}{L_i} \bar{v}_{i,j} & \text{if } \bar{p} = \bar{s} \text{ and } (i = N \text{ or } m_{i+1} \leq j \leq M_{i+1}) \\ \frac{T}{L_i} \bar{v}_{i,j} & \text{if } \bar{p} > H_0 \text{ and } \bar{s} = \bar{p} - M_{i-1} + m_i - 1 \\ 0 & \text{otherwise} \end{cases} \quad (7)$$

$$b_{\bar{p},\bar{s}} = \begin{cases} \frac{T}{L_i} & \text{if } j > m_i \text{ and } \bar{s} = \bar{p} - i \\ -\frac{T}{L_i} & \text{if } j < M_i \text{ and } \bar{s} = \bar{p} - i + 1 \\ \frac{T}{L_i} & \text{if } j = \bar{j} \text{ and } i = \bar{i} \\ 0 & \text{otherwise} \end{cases} \quad (8)$$

where  $(\bar{i}, \bar{j})$  defines the location of on-ramp flow.

Finally, note that the CFL condition [13]

$$\frac{T}{L_i} \bar{v} < 1 \quad (9)$$

should be respected for a realistic discrete time and discrete space traffic flow model.

### III. LATERAL FLOW AND RAMP METERING CONTROLLER

#### A. Formulation

We employ here the linear system described in Section II to formulate an optimal control problem, whose solution leads to a MIMO (multi-input multi-output) feedback controller. Specifically, the controller should manipulate the lateral flows, as well as the flow entering from an on-ramp located upstream of the bottleneck, with the goals of avoiding the creation of congestion and indeed maximising the bottleneck throughput.

To maximise the bottleneck throughput, densities at the bottleneck areas should be maintained around their critical values ( $\rho_{S \times 1}^{cr}$ ), which are here supposed to be known. In presence of disturbances (e.g., upstream mainstream demand or uncontrolled lateral flows), in order to avoid offset at the stationary state, we employ an integral controller to reject constant disturbances [14], thus removing the need for measuring the external inflows. We formulate our problem by augmenting the original system (3) with  $S$  (i.e., as many as bottleneck lanes) integral states, denoted as  $z$ , where

$$z(k+1) = z(k) + \bar{C}\bar{x}(k) - \rho^{cr}. \quad (10)$$

The resulting augmented system reads

$$x(k+1) = Ax(k) + Bu(k) + d(k), \quad (11)$$

where

$$x = \begin{bmatrix} \bar{x} \\ z \end{bmatrix}, \quad d = \begin{bmatrix} \bar{d} \\ -\rho_{S \times 1}^{cr} \end{bmatrix}, \quad A = \begin{bmatrix} \bar{A} & 0_{H \times S} \\ \bar{C} & I_{S \times S} \end{bmatrix}, \quad (12)$$

$$B = \begin{bmatrix} \bar{B} \\ 0_{S \times (F+1)} \end{bmatrix}, \quad \bar{C} = [0_{S \times (H-S)} \quad I_{S \times S}]. \quad (13)$$

We define the following quadratic cost function, over an infinite time horizon, which accounts for penalization of integral states and control inputs:

$$J = \sum_{k=0}^{\infty} [x^T(k) C Q C^T x(k) + u^T(k) R u(k)], \quad (14)$$

where

$$Q = w_Q I_{S \times S}, \quad R = \begin{bmatrix} w_{R_1} I_{F \times F} & 0_{F \times 1} \\ 0_{1 \times F} & w_{R_2} \end{bmatrix} \quad (15)$$

$$C = [0_{S \times H} \quad I_{S \times S}]. \quad (16)$$

Matrices  $Q$  and  $R$  are weighting matrices associated to the magnitude of the integral states and control actions, respectively, defined by parameters  $w_Q > 0$ ,  $w_{R_1} > 0$ , and  $w_{R_2} > 0$ . The optimal control problem associated to (14), (11) can be solved through a Linear Quadratic Regulator (LQR), which provides a stabilising feedback gain under the assumptions that the original system is, at least, stabilisable and detectable (see Chapter 2 of [15]), which can be verified using, e.g, the Hautus-test [16]. The system matrix  $A$  in (11) is, by construction, lower triangular, implying that its eigenvalues  $\lambda$  are equal to the elements in the main diagonal. Assuming (9) is respected and  $\bar{v}$  is always positive, the modes related to segments for which another downstream segment exists are always stable ( $|\lambda| < 1$ ), while the modes related to segments without any other segment downstream (i.e., at a lane-drop), as well as the integral state modes, are marginally stable ( $\lambda = 1$ ).

To guarantee that the pair  $(A, B)$  is stabilisable,  $B$  must have more linearly independent columns than the number of non-stable ( $\lambda \geq 1$ ) modes. In case there are no lane-drops, there are  $S$  marginally stable modes, corresponding to integral states, which, in order to satisfy the condition, require at least  $S$  control inputs. Since, in our system configuration, there are at least  $S - 1$  lateral flows (i.e., the lateral flows at the bottleneck location), and an on-ramp input, the stabilisability condition is satisfied.

We turn now our attention to the detectability of the pair  $(A, C^TQC)$  in (14); according to [17], since  $Q > 0$ , this is equivalent to investigating the detectability of the pair  $(A, C)$ . This is verified, in case there are no lane-drops, when controlling all integral states. Since, the pair  $(A, C)$  satisfies criteria in [16].

### B. Controller design

The solution to the proposed LQR problem is the linear feedback control law

$$u(k) = -Kx(k), \quad (17)$$

where

$$K = (R + B^T P B)^{-1} B^T P A \quad (18)$$

$$P = C^T Q C + A^T P A - A^T P B (R + B^T P B)^{-1} \quad (19)$$

The optimal gain (18) and the Algebraic Riccati Equation (19) can be found in classic Optimal Control books [18]. The feedback control law (17) is very effective for practical application since the computation of the feedback gain matrix  $K$  may be affected offline. For practical implementation, the gain  $K$  can be appropriately split as

$$K = [ K_P \quad K_I ], \quad (20)$$

which allows to compute the control law as

$$u(k) = -K_P \bar{x}(k) - K_I z(k). \quad (21)$$

In practice, it may not be always possible to achieve the desired density set-point at the bottleneck (e.g., due to input saturation), therefore it is necessary to include an

anti-windup scheme in our controller. We employ the one proposed in [19] (see also [20], [21]), which, in our case, modifies the integral part of the dynamic controller (10) as

$$z(k+1) = (I + MK_I)z(k) + (\bar{C} + MK_P)x(k) + Mu_{\text{sat}}(k). \quad (22)$$

The saturated input  $u_{\text{sat}}$  is defined as follows

$$u_{\text{sat}}(k) = \text{sat}(u(k)) \quad (23)$$

$$\text{sat}(u_m) = \begin{cases} u_m^{\min} & \text{if } u_m < u_m^{\min} \\ u_m^{\max} & \text{if } u_m > u_m^{\max} \\ u_m, & \text{otherwise,} \end{cases} \quad (24)$$

where  $m$  is the index of the element inside vector  $u$ , and  $u_m^{\min}$  and  $u_m^{\max}$  are the lower and upper bound for the input  $u_m$ . Respectively, matrix  $M$  should be chosen so that  $I + MK_I$  has stable eigenvalues, for example, via classical pole placement. Note that, when inputs are not saturated, equation (22) becomes (10), which is stable according to our results in III-A, while, when inputs are saturated, as  $M$  makes stable eigenvalues for (22), again the system is stable [22].

## IV. EXPERIMENT SETUP

### A. Nonlinear multi-lane traffic flow model

In order to test and evaluate the performance of the proposed control strategy, we present simulation experiments using a first-order traffic flow model based on [7]. The model is used for reproducing the traffic behaviour for a multi-lane motorway and it features: (i) non-linear functions for the lateral flows of manually driven vehicles (which may also act as disturbances for the designed controller); (ii) a Cell Transmission Models (CTM)-like formulation for the longitudinal flows; and (iii) a non-linear formulation to account for the capacity drop phenomenon. Briefly, we consider the conservation law equation (1), where all variables are defined as in Section II. Lateral flows due to manual lane-changing, denoted as  $\bar{f}_{i,j}^M(k)$  are considered among adjacent lanes of the same segment, and corresponding rules are defined in order to properly assign and bound their values. They are computed as

$$\bar{f}_{i,j}^M(k) = l_{i,j,j+1}(k) - l_{i,j+1,j}(k), \quad (25)$$

where

$$l_{i,\bar{j},j}(k) = \min \left\{ 1, \frac{E_{i,j}(k)}{D_{i,j-1,j}(k) + D_{i,j+1,j}(k)} \right\} D_{i,\bar{j},j}(k) \quad (26)$$

$$E_{i,j}(k) = \frac{L_i}{T} [\rho_{i,j}^{\text{jam}} - \rho_{i,j}(k)] \quad (27)$$

$$D_{i,j}(k) = \frac{L_i}{T} \rho_{i,j}(k) A_{i,j,\bar{j}}(k) \quad (28)$$

$$A_{i,j,\bar{j}}(k) = \mu \max \left\{ 0, \frac{G_{i,j,\bar{j}}(k) \rho_{i,j}(k) - \rho_{i,\bar{j}}(k)}{G_{i,j,\bar{j}}(k) \rho_{i,j}(k) + \rho_{i,\bar{j}}(k)} \right\}, \quad (29)$$

and  $\bar{j} = j \pm 1$ .  $E$  denotes the available space, in terms of flow acceptance, while  $D$  denotes the lateral demand flow, which is computed via definition of the attractiveness rate  $A$ . Equation (26) accounts for the potentially limited space that

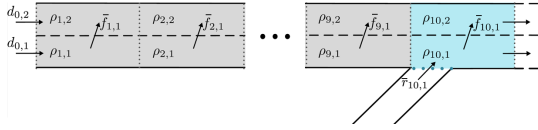


Fig. 2: Motorway stretch employed in the simulation experiments.

may not be sufficient for accepting the lateral flow entering from both sides of a cell. In (29), the factor  $G$  is mostly equal to 1, which implies the intent of drivers to move towards a faster lane (leading also to equal densities among lanes), but may also be tuned to reflect particular location-dependent effects where lateral flow may occur in the direction from a lower density to a higher one (e.g. upstream of on- and off-ramps, lane drop locations, etc.); while  $\mu$  is a constant coefficient in the range  $[0, 1]$  reflecting the “aggressiveness” in lane-changing.

Longitudinal flows are the flows going from a cell to the next downstream one, while remaining in the same lane. We employ the Godunov-discretised first-order model proposed in [7], employing however a non-linear exponential demand function for under-critical densities, to obtain a more realistic behaviour at low densities. The model accounts also for the capacity drop phenomenon, via a linearly decreasing demand function for over-critical densities and a linear reduction of the maximum flow as a function of the entering lateral flows [23]. The overall formulation for longitudinal flow is

$$q_{i,j}(k) = \min \{ Q_{i,j}^D(k), Q_{i+1,j}^E(k) - d_{i,j}(k) \}, \quad (30)$$

where

$$Q_{i,j}^D(k) = \begin{cases} v_{i,j}^{\max} \exp \left[ -\frac{1}{\alpha} \left( \frac{\rho_{i,j}(k)}{\rho_{i,j}^{\text{cr}}} \right)^\alpha \right] \rho_{i,j}(k), & \text{if } \rho_{i,j}(k) < \rho_{i,j}^{\text{cr}} \\ \frac{(1-\gamma)Q_{i,j}^{\text{cap}}}{\rho_{i,j}^{\text{cr}} - \rho_{i,j}^{\text{jam}}} \left[ \rho_{i,j}(k) - \rho_{i,j}^{\text{jam}} \right] + Q_{i,j}^B(k), & \text{otherwise} \end{cases} \quad (31)$$

$$Q_{i+1,j}^E(k) = \begin{cases} Q_{i+1,j}^{\text{cap}}, & \text{if } \rho_{i+1,j}(k) < \rho_{i+1,j}^{\text{cr}} \\ w_{i+1} \left[ \rho_{i+1,j}^{\text{jam}} - \rho_{i+1,j}(k) \right], & \text{otherwise.} \end{cases} \quad (32)$$

$$Q_{i,j}^B(k) = \gamma Q_{i,j}^{\text{cap}} - \eta [l_{i,j+1,j}(k) + l_{i,j-1,j}(k)] \quad (33)$$

Parameter  $v^{\max}$  denotes the maximum speed,  $Q^{\text{cap}}$  is the capacity flow,  $\rho^{\text{cr}}$  is the critical density (i.e., the density at which the capacity flow occurs), while  $\alpha = \left( \ln \frac{Q^{\text{cap}}}{v^{\max} \rho^{\text{cr}}} \right)^{-1}$  [24]. Parameter  $\gamma$  influences the impact of capacity drop due to overcritical densities, while  $\eta$  affects the capacity drop due to entering lateral flows. Note that, setting  $\gamma = 1$  and  $\eta = 0$ , we obtain a conventional first-order model, i.e. no capacity drop appears at the head of congestion.

### B. Network description and simulation configuration

We consider a hypothetical two-lane motorway stretch, shown in Fig. 2, to test and evaluate the performance of the proposed strategy. In particular, we consider a network composed of 10 segments characterised by the same length

TABLE I: Parameters used in the nonlinear multi-lane traffic flow model.

	$v^{\max}$	$Q^{\text{cap}}$	$\rho^{\text{cr}}$	$\rho^{\text{jam}}$	$\gamma$	$\eta$	$G$	$\mu$
	[km/h]	[veh/h]	[veh/km]	[veh/km]				
$j=1$	100	1800	22	120	0.6	0.8	1	0.6
$j=2$	100	2400	26	160	0.6	0.8	1	0.6

$L_i = 0.5$  km, while we employ a time step  $T = 10$  s. Different lanes feature different parameters, namely a different FD, which may reflect different traffic composition (e.g., a high number of heavy vehicles reducing the capacity of a specific lane). In addition, the used traffic demand is depicted in Fig. 3.

We introduce variable  $\Phi^{\text{crt}}(k)$  to indicate if the controller is active at time  $k$  ( $\Phi^{\text{crt}}(k) = 1$ ) or not ( $\Phi^{\text{crt}}(k) = 0$ ), which reflects how the lateral flows are computed in our simulation experiments. In addition, while applying our controller, we assume that 50 % of the vehicles are connected and automated, therefore a percentage of the manual lane-changing flow is included as additive noise. Different percentage of automated vehicles is studied and the results will appear in future publication which denotes, higher percentage of automated vehicles results in lower TTS. The lateral flow implemented in our simulations is therefore

$$\bar{f}_{i,j}(k) = \begin{cases} \bar{f}_{i,j}^M(k), & \text{if } \Phi^{\text{crt}}(k) = 0, \\ \text{sat}(f_{i,j}(k)) + 0.5 \bar{f}_{i,j}^M(k), & \text{if } \Phi^{\text{crt}}(k) = 1. \end{cases} \quad (34)$$

Since ramp metering actions may create a queue outside the motorway network, we introduce the following dynamics for the queue length  $w(k)$  (in veh).

$$w(k+1) = w(k) + T(g_{10,1}(k) - r_{10,1}(k)), \quad (35)$$

where  $g_{10,1}(k)$  is the on-ramp demand during time interval  $(k, k+1]$ . The ramp flow implemented in our simulations is

$$\bar{r}_{10,1}(k) = \begin{cases} g_{10,1}(k), & \text{if } \Phi^{\text{crt}}(k) = 0, \\ \text{sat}(r_{10,1}(k)), & \text{if } \Phi^{\text{crt}}(k) = 1. \end{cases} \quad (36)$$

Note that we consider the following bounds for the control inputs:

$$\text{sat}(f_{i,j}) = \begin{cases} f_{i,j}^{\min} = -\frac{L_i}{T} \rho_{i,j} & \text{if } f_{i,j} \leq f_{i,j}^{\min} \\ f_{i,j}^{\max} = \frac{L_i}{T} \rho_{i,j} & \text{if } f_{i,j} \geq f_{i,j}^{\max} \\ f_{i,j}, & \text{otherwise;} \end{cases} \quad (37)$$

$$\text{sat}(r_{10,1}) = \begin{cases} r_{10,1}^{\min} = 0, & \text{if } r_{10,1} \leq r_{10,1}^{\min} \\ r_{10,1}^{\max} = \min\left(\frac{w}{T} + D_{10,1}, Q_1^{\text{cap}}\right), & \text{if } r_{10,1} \geq r_{10,1}^{\max} \\ r_{10,1}, & \text{otherwise.} \end{cases} \quad (38)$$

## V. EXPERIMENTAL RESULTS

### A. No-control case

The no-control case is defined by implementation of the nonlinear traffic model (25)-(33) in the described network.

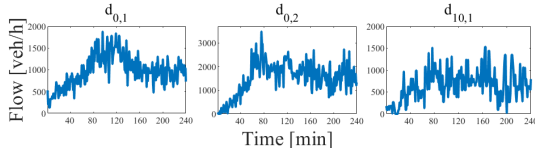


Fig. 3: Traffic demand used in the simulation experiments.

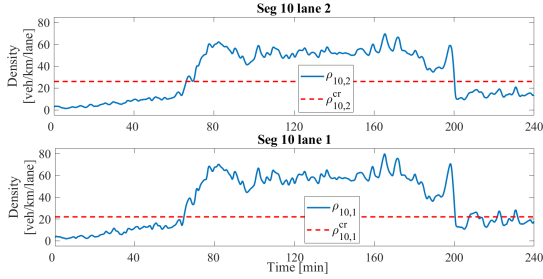


Fig. 4: Density in the no-control case.

Looking at Figs. 4 and 5, one may observe that a strong congestion develops at the merge area (segment 10) and spills-back until segment 1. The reasons for the congestion are a) the high inflow entering from the ramp, since the total demand during the peak period is about 4600 veh/h, while the overall capacity is 4200 veh/h; as well as b) the inefficient “natural” lane-changing flow. Capacity drop also occurs at the bottleneck cells of the stretch, which worsens the congestion.

### B. Lateral flow and ramp metering controller

We employ the linear dynamic compensator (21), (22) to the non-linear traffic model (25)-(33). We performed a set of experiments to evaluate the sensitivity of the controller to the choice of parameters  $w_Q$ ,  $w_{R_1}$  and  $w_{R_2}$ , and we observed that the controller has good performance, in term of Total Time Spent (TTS), calculated as in [25], for a wide range of parameter values. We show here results using  $w_Q = 1$ ,  $w_{R_1} = 1$  and  $w_{R_2} = 0.001$ . Congestion fully disappears and the densities at the bottleneck area remain at their critical values, see Figs. 6 and 7. Control outputs are computed so that critical density is not exceeded and they are suggested for the entire duration of the simulation experiment. On the other hand, a large queue is created at the on-ramp during the peak period, which is not upper-bounded in our experiments (see Fig. 9). The TTS improvement is about 26% (see also Table II).

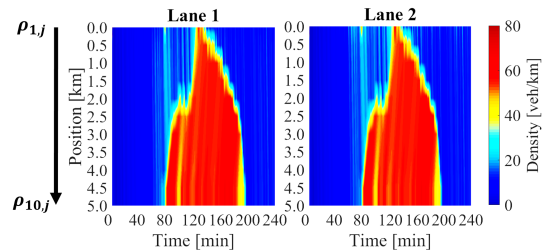


Fig. 5: Contour plots of densities in the no-control case.

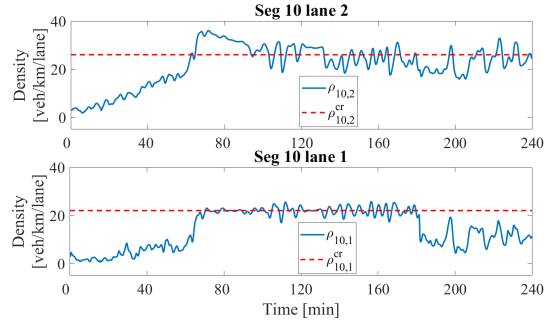


Fig. 6: Density in the controlled case.

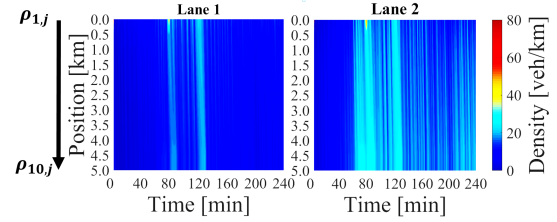


Fig. 7: Contour plots of densities in the controlled case.

### C. Implementation of an activation logic

It is not necessary nor reasonable at low densities (far from  $\rho^{cr}$ ) to order lane-changing of vehicles, since it is not likely that a congestion would occur. In this experiment we introduce an activation and deactivation logic as follows

$$\begin{cases} \Phi^{crt}(k) = 1, & \text{if } \sum_j \rho_{I,j}(k) > \rho^{act} \\ \Phi^{crt}(k) = 0, & \text{if } \sum_j \rho_{I,j}(k) < \rho^{deact} \\ \Phi^{crt}(k) = \Phi^{crt}(k-1), & \text{if } \rho^{deact} < \sum_j \rho_{I,j}(k) < \rho^{act} \end{cases} \quad (39)$$

where  $\rho^{act}$  and  $\rho^{deact}$ , are the activation and deactivation threshold, respectively. We consider selecting  $\rho^{act} > \rho^{deact}$  in order to avoid switches between activation and deactivation states. In our experiments, we choose  $\rho^{act}$  as

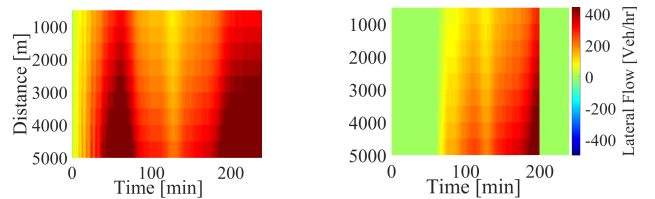


Fig. 8: Contour plots of lateral flows in the controlled case; without activation logic (left) and with activation logic (right).

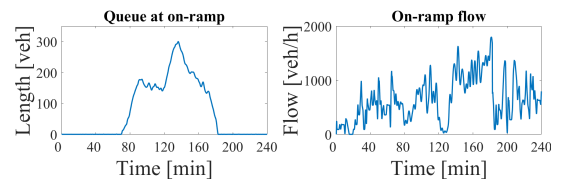


Fig. 9: Ramp queue (left) and ramp flow (right) in the controlled case.

TABLE II: TTS for the different scenarios.

	No control case	Without activation logic	With activation logic
TTS [hr]	1060	783	810
Improvement (%)		26	23

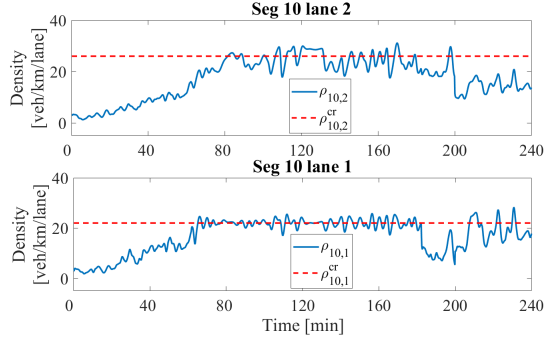


Fig. 10: Density in the controlled case with activation logic.

$0.7 \sum_{j=1}^2 \rho_{10,j}^{cr}$  and  $\rho^{deact}$  as  $0.5 \sum_{j=1}^2 \rho_{10,j}^{cr}$ . Similarly as in previous case, using the activation logic, the congestion fully disappears and the densities at the bottleneck area remain at their critical values, see Figs. 10 and 11. Also, from Fig. 8 (right), the controller is activated only in the middle of the simulation. Namely when in the no-control case the congestion was create. The TTS improvement is about 23% (see Table II).

## VI. CONCLUSIONS

This paper presents a novel methodology for integrated lane-changing and ramp metering control at motorway bottlenecks, which accounts for the presence of connected and partly automated vehicles. The method is evaluated via simulation experiments, through a first-order, multi-lane, macroscopic traffic flow model featuring the capacity drop phenomenon, which allows to show the effectiveness of the developed methodology. We are currently investigating stability properties of the controller, as well as producing further simulation experiments to investigate robustness to parameter choices and to different type of disturbances, which are going to appear in a future publication.

## REFERENCES

[1] R. Bishop, *Intelligent vehicle technology and trends*. Artech House Publishers, 2005.

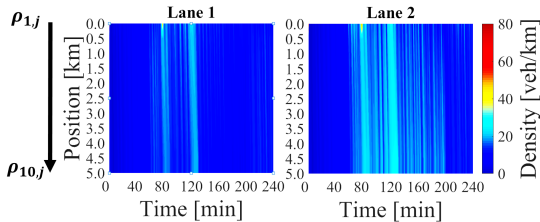


Fig. 11: Contour plots of densities, in the controlled case, with activation logic.

[2] C. Diakaki, M. Papageorgiou, I. Papamichail, and I. K. Nikolos, "Overview and analysis of vehicle automation and communication systems from a motorway traffic management perspective," *Transportation Research Part A*, vol. 75, pp. 147 – 165, 2015.

[3] A. Ghaffari, A. Khodayari, A. Kamali, F. Tajdari, and N. Hosseinkhani, "New fuzzy solution for determining anticipation and evaluation behavior during car-following maneuvers," *Proceedings of the Institution of Mechanical Engineers, Part D: Journal of Automobile Engineering*, vol. 232, pp. 936–945, 2018.

[4] A. Ghaffari, A. Khodayari, A. Kamali, and F. Tajdari, "A New Model of Car Following Behavior Based on Lane Change Effects using Anticipation and Evaluation Idea," *Iranian Journal of Mechanical Engineering*, vol. 16(2), pp. 26–38, 2015.

[5] R. W. Hall and D. Lospitch, "Optimized lane assignment on an automated highway," *Transportation Research Part C*, vol. 4, no. 4, pp. 211–229, 1996.

[6] K. Kim, J. V. Medanić, and D. I. Cho, "Lane assignment problem using a genetic algorithm in the Automated Highway Systems," *International Journal of Automotive Technology*, vol. 9, no. 3, pp. 353–364, 2008.

[7] C. Roncoli, M. Papageorgiou, and I. Papamichail, "Traffic flow optimisation in presence of Vehicle Automation and Communication Systems - Part II: Optimal control for multi-lane motorways," *Transportation Research Part C*, vol. 57, pp. 260 – 275, 2015.

[8] Y. Zhang and P. A. Ioannou, "Combined variable speed limit and lane change control for highway traffic," *IEEE Transactions on Intelligent Transportation Systems*, vol. 7, pp. 1812–1823, 2017.

[9] C. Roncoli, N. Bekiaris-Liberis, and M. Papageorgiou, "Optimal lane-changing control at motorway bottlenecks," *IEEE 19th International Conference on Intelligent Transportation Systems (ITSC)*, pp. 1785–1791, 2016.

[10] C. Roncoli, M. Papageorgiou, and N. Bekiaris-Liberis, "Lane-changing feedback control for efficient lane assignment at motorway bottlenecks," *Transportation Research Record*, vol. 2625, pp. 20–31, 2017.

[11] F. Tajdari, E. Khodabakhshi, M. Kabganian, and A. Golgouneh, "Switching controller design to swing-up a two-link underactuated robot," *2017 IEEE 4th International Conference on Knowledge-Based Engineering and Innovation (KBEI)*, pp. 0595 – 0599, 2017.

[12] C. Roncoli, M. Papageorgiou, and I. Papamichail, "Traffic flow optimisation in presence of Vehicle Automation and Communication Systems - Part I: A first-order multi-lane model for motorway traffic," *Transportation Research Part C*, vol. 57, pp. 241 – 259, 2015.

[13] R. Courant, K. Friedrichs, and H. Lewy, "Über die partiellen differenzgleichungen der mathematischen physik," *Mathematische Annalen*, vol. 100, no. 1, pp. 32–74, 1928.

[14] K. J. Åström and T. Häggglund, *PID controllers: theory, design, and tuning*, 1995.

[15] F. L. Lewis, D. L. Vrabie, and V. L. Szymos, *Optimal Control*. John Wiley & Sons, Inc., 2012.

[16] R. L. Williams and D. A. Lawrence, *Linear state-space control systems*. Hoboken, NJ, USA: John Wiley & Sons, Inc., 2007.

[17] J. P. Hespanha, *Linear Systems Theory*, 2009.

[18] B. D. O. Anderson and J. B. Moore, *Linear optimal control*. Prentice-Hall, 1971.

[19] K. J. Åström and L. Rundqwist, "Integrator Windup and How to Avoid It," *1989 American Control Conference*, 1989.

[20] M. V. Kothare, P. J. Campo, M. Morari, and C. N. Nett, "A unified framework for the study of anti-windup designs," *Automatica*, vol. 30, no. 12, pp. 1869–1883, 1994.

[21] N. Kapoor, A. R. Teel, and P. Daoutidis, "An Anti-Windup Design for Linear Systems with Input Saturation," *Automatica*, vol. 34, no. 5, pp. 559–574, 1998.

[22] J. G. da Silva Jr and S. Tarbouriech, "Anti-windup design with guaranteed regions of stability for discrete-time linear systems," *Systems & Control Letters*, vol. 55, no. 3, pp. 184–192, 2006.

[23] M. Kontorinaki, A. Spiliopoulou, C. Roncoli, and M. Papageorgiou, "First-order traffic flow models incorporating capacity drop: Overview and real-data validation," *Transportation Research Part B*, vol. 106, pp. 52–75, 2017.

[24] A. Messmer and M. Papageorgiou, "METANET: A macroscopic simulation program for motorway networks," *Traffic Engineering and Control*, vol. 9, pp. 466–470, 1990.

[25] M. Papageorgiou, C. Diakaki, V. Dinopoulou, A. Kotsialos, and Y. Wang, "Review of road traffic control strategies," in *Proceedings of the IEEE*, vol. 91, 2003, pp. 2043–2065.